arXiv:1611.07259v2 [hep-ex] 27 Jan 2017

Constraints on Scalar-Pseudoscalar and Tensorial Non-Standard Interaction and Tensorial Unparticle Couplings from Neutrino-Electron Scattering

M. Deniz,[1,2,3,*] B. Sevda,[1,2] S. Kerman,[1,2] A. Ajjaq,[1] L. Singh,[2,4] H.T. Wong,[2] and M. Zeyrek[3]

[1] *Department of Physics, Dokuz Eylül University, Buca, İzmir TR35160, Turkey*
[2] *Institute of Physics, Academia Sinica, Taipei 115, Taiwan*
[3] *Department of Physics, Middle East Technical University, Ankara TR06531, Turkey*
[4] *Department of Physics, Banaras Hindu University, Varanasi 221005, India*

(Dated: January 30, 2017)

Neutrino-electron scattering is a purely leptonic fundamental interaction and therefore provides an important channel to test Standard Model (SM) especially at the low energy-momentum transfer regime. We derived constraints on neutrino Non-Stardard-Interactions (NSI) couplings depending on model independent approaches which are described by a four-Fermi point like interaction and Unparticle Physics model with tensorial components. Data on $\bar{\nu}_e - e$ and $\nu_e - e$ scattering from the TEXONO and LSND experiments, respectively, are used. The upper limits and the allowed regions of scalar, pseudoscalar and tensorial NSI couplings of neutrinos are derived at 90% confidence level in both one-parameter and two-parameter analysis. New upper limits for tensorial unparticle physics coupling constants and mass parameters are also placed.

I. INTRODUCTION

The discovery of neutrino oscillations undoubtedly shows that neutrinos have tiny but nevertheless non-zero mass. Recent developments in neutrino physics such that the discovery of existence of neutrino mass via oscillation phenomena and intense experimental efforts to reveal properties of neutrinos show that neutrinos still play very important role in particle physics and therefore they are keystones for completeness of the SM [1]. Solar and Atmospheric experimental data have confirmed that neutrinos do oscillate, thereby they are massive and can be mixed. Extra new interactions due to nonstandard properties of neutrinos which are often called nonstandard interaction (NSI) of neutrino have not been observed experimentally yet, mainly due to poor experimental sensitivities.

Recent and upcoming neutrino experiments will provide more precise measurements on intrinsic neutrino properties [2], therefore, have potential to open a new window for observation of NSI effects [3]. Non-oscillation experiments that have measured neutrino cross section with high accuracy may provide profound information for neutrino interactions resulting in direct measurements of NSI. These interactions are important not only for phenomenological [4], but also for experimental point of view since the measurements and found evidences can suggest new physics or favor one of the existing new physics theories BSM.

Neutrino-electron scattering provides quite convenient channel for testing the SM of electroweak theory especially in low energy regime since it is a pure leptonic process [5–9]. Advanced systems capable of making measurements at low energy-low background are necessary to observe neutrino interactions with a good experimental precision. In principle, there are some advantages to study with reactor neutrinos ($\bar{\nu}_e$): The reactors are excellent sources for low energy electron type antineutrino with high neutrino flux up to around 10 MeV. Besides reactor ON and OFF comparison providing model-independent way of background subtraction, the reactor $\bar{\nu}_e$ spectra is understood and well known. Therefore, these advantages provide better experimental sensitivities.

This paper is a follow-up of our earlier studies on (i) Non-Universal or Flavor Conserving (FC) and Flavor-Changing or Flavor-Violating (FV) NSI of neutrino, and (ii) vector and scalar unparticle physics (UP) [6]. We report experimental constraints on scalar, pseudoscalar, and tensorial NSI and tensorial unparticle couplings via neutrino-electron elastic scattering interaction channels.

II. NEUTRINO-ELECTRON SCATTERING AND DATA

A. Standard Model

$\nu_e(\bar{\nu}_e) - e$ elastic scattering can occur via both charged current and neutral current. Therefore, their interference which is destructive also contributes to the cross section. The SM differential cross section of $\nu_e(\bar{\nu}_e) - e$ elastic scattering can be expressed in terms of chiral coupling of g_L and g_R in the laboratory frame as [6, 10]

$$\left[\frac{d\sigma}{dT}(\nu_e e)\right]_{\rm SM} = \frac{2G_F^2 m_e}{\pi}\left[(g_L+1)^2 + g_R^2\left(1-\frac{T}{E_\nu}\right)^2 - g_R(g_L+1)\frac{m_e T}{E_\nu^2}\right], \quad (1)$$

* Corresponding Author: muhammed.deniz@deu.edu.tr

and

$$\left[\frac{d\sigma}{dT}(\bar{\nu}_e e)\right]_{\rm SM} = \frac{2G_F^2 m_e}{\pi}\left[g_R^2 + (g_L+1)^2\left(1-\frac{T}{E_\nu}\right)^2 - g_R(g_L+1)\frac{m_e T}{E_\nu^2}\right], \quad (2)$$

where G_F is the Fermi coupling constant, T is the kinetic energy of the recoil electron, E_ν is the incident neutrino energy, and $g_L = -\frac{1}{2} + sin^2\theta_W$ and $g_R = sin^2\theta_W$ are the chiral coupling constants in terms of weak mixing angle $sin^2\theta_W$.

B. Input Data

Short-baseline neutrino experiments provide some advantages to study BSM. Due to minimizing oscillation effect short-baseline reactor neutrino experiments, where pure $\bar{\nu}_e$ is produced unlike mixing of different eigenstates of neutrinos as in the case of Solar and Atmospheric ones, can be used to probe BSM effectively. Reactors produce high $\bar{\nu}_e$ fluxes compared to other sources. The Reactor-OFF period provides model-independent means of background subtraction. The studies of reactor $\bar{\nu}_e - e$ interaction provide better sensitivities to the SM electroweak parameters $\sin^2\theta_W$ and g_V, g_A at the same experimental accuracies as those from ν_e measurements [11]. The lower neutrino energy at the MeV range also favors applications where sensitivities can be enhanced at low detector thresholds.

In this paper, the analyses of the experimental data sets of TEXONO as a sample of antineutrino channel at low energy with three different detectors located at Kuo-Sheng Reactor Neutrino Laboratory (KSNL) whose energy ranges are different and LSND Experiment as a sample of neutrino channel at high energy are reported. The results from tree independent data sets from TEXONO of $\bar{\nu}_e$ − e interaction are compared with those from the data set of LSND ν_e − e interaction.

KSNL is located at a distance of 28 m from one of the cores of Nuclear Power Plant in Taiwan with 30 meter-water-equivalent overburden. The 2.9 GW reactor cores are produced an average $\bar{\nu}_e$ flux of $\phi(\bar{\nu}_e) \sim 6.4 \times 10^{12}$ cm^{-2}s^{-1} at the experimental site. Detectors were placed inside the laboratory that is equipped with a 50-ton passive shielding materials together with surrounding active detectors: Cs(Tl) or NaI(Tl) for anti-Compton detector, and a cosmic-ray veto scintillator array.

TEXONO Experiment: Three experimental data sets taken with different detectors are used as follows:

CsI(Tl): 29882/7369 kg-days of Reactor ON/OFF data: $\bar{\nu}_e - e^-$ electroweak interaction cross section, g_V, g_A, weak mixing angle $sin^2\theta_W$ and charge radius squared were measured with an effective mass of 187 kg CsI(Tl) crystal scintillator array at 3 − 8 MeVee. The RMS energy resolutions are 5.8%, 5.2%, and 4.0% at ^{137}Cs, ^{40}K, and ^{208}Tl γ peaks, respectively [11].

HP-Ge: 570.7/127.8 kg-days of Reactor ON/OFF data: New limits are set to neutrino magnetic moment and axion with a target mass of 1.06 kg high-purity germanium detector [12] at 12 − 64 keVee. The RMS energy resolution of HP-Ge is 880 keVee at Ga-K shell X-ray energy [13].

PC-Ge: 124.2/70.3 kg-days of Reactor ON/OFF data: New limits are set to neutrino millicharge and low mass WIMP with a fiducial mass of 500 g point contact germanium (PC-Ge) detector [8] at 0.3 − 12 keVee energy region. The RMS energy resolution of PC-Ge is 87 keVee at Ga-K shell X-ray energy [13].

LSND Experiment: Liquid Scintillator Detector at the Los Alamos Neutron Science Center using neutrinos produced at the proton beam stop with T of 18 − 50 MeVee. The cross section for the elastic scattering reaction $\nu_e - e$ and weak mixing angle $sin^2\theta_W$ were measured. The energy resolution was determined from the shape of the electron energy spectrum and was found to be 6.6% at the 52.8 MeV end point [14].

C. Analysis Methods

FC and FV NSI, as well as scalar and vector UP were studied in our previous studies by using the data sets of CsI(Tl) and HP-Ge [6]. In this paper, we adopt the same analysis methods for the new interaction channels. A new data set of PC-Ge of TEXONO is also included for the analysis to cover lower energy range as well.

The expected event rate of R can be calculated as

$$R_X = \rho_e \int_T \int_{E_\nu} \left[\frac{d\sigma}{dT}\right]'_X \frac{d\phi(\bar{\nu}_e)}{dE_\nu}\, dE_\nu\, dT \quad , \quad (3)$$

where ρ_e is the electron number density per kg of target mass, and $d\phi/dE_\nu$ is the neutrino spectrum. The measurable differential cross-section is denoted by $[d\sigma/dT]'$ which corresponds to convoluting the detector energy resolution to the physics differential cross-section $[d\sigma/dT]$. In practice, for the BSM models and experimental data studied in this work, the variations of $[d\sigma/dT]$ with energy are gradual, such that the resolution smearing does not significantly alter the measured spectra in the region of interest. The difference between $[d\sigma/dT]$ and $[d\sigma/dT]'$ is less than 0.1%. Accordingly, resolution effects can be neglected in this analysis.

R_{expt} and R_X correspond to observed and expected event rates, respectively. X represents different interaction channel such as SM, NSI, etc. R_{expt} is expressed in

the unit of $kg^{-1}MeV^{-1}day^{-1}$ and $kg^{-1}keV^{-1}day^{-1}$ for CsI(Tl) and Ge data sets, respectively.

The results on physics couplings from this analysis are expressed either as "best-fit ± statistical ± systematic uncertainties" at 1-σ level, or in terms of limits at 90% Confidence Level (CL). The statistical uncertainties are derived by minimum χ^2 method defined as

$$\chi^2 = \sum_{i=1} \left[\frac{R_{expt}(i) - R_{SM}(i) - R_X(i)}{\Delta(i)} \right]^2 , \qquad (4)$$

where R_{expt}, R_{SM} and R_X are measured event rate, SM and X (= NSI, UP, etc.) expected event rates, respectively, while $\Delta(i)$ is the statistical uncertainty of the i-th bin published by the experiments. The 1-σ statistical errors in the physics couplings correspond to those values that produce $\chi^2 = \chi^2_{min} + 1$. The published systematic uncertainties of the experiments contribute to shifts of the best-fit values in the physics couplings. The two contributions are added in quadrature to give rise to the combined uncertainties, from which the 90% CL limits can be derived using the prescription of Ref. [15].

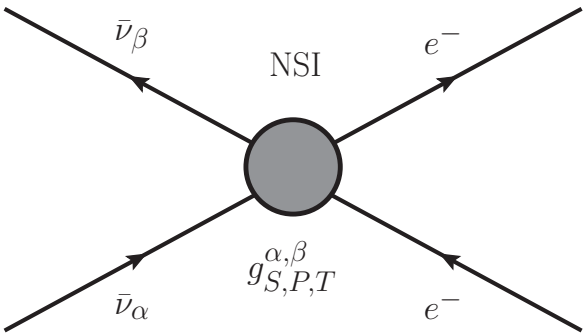

Figure 1. NSI of neutrinos, generically described as four-Fermi interaction with new couplings.

III. SCALAR, PSEUDO-SCALAR AND TENSORIAL NSI OF NEUTRINO

Since neutrino-electron scattering is pure leptonic process, it provides very convenient channel to test the SM. NSI of neutrinos is first considered as an alternative mechanism for neutrino oscillation. However, NSI is now only allowed for lower pioneers effects to the neutrino oscillation and can be used to improve the sensitivities of oscillation experiments. In this report, investigation of some of the BSM new physics scenarios via $\nu_e(\bar{\nu}_e)-e$ elastic scattering is introduced and the results will be given in subsequent sections. In these new physics scenarios, the NSI of neutrinos is considered as a model independent interaction which is described as four-Fermi point

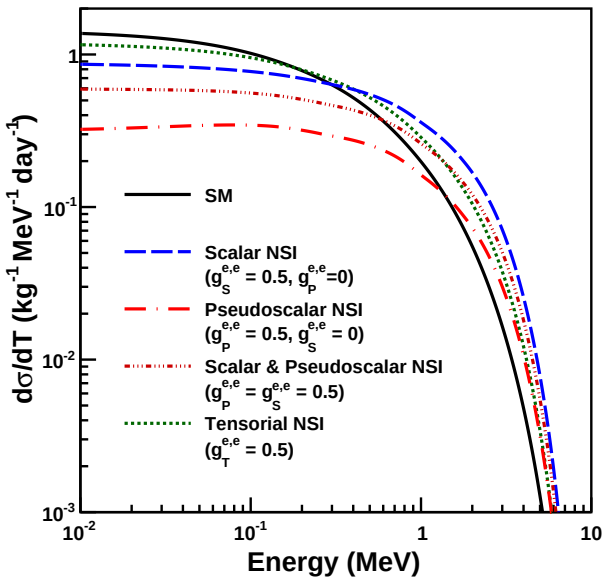

Figure 2. (color online). Differential cross section as a function of the recoil energy T with typical reactor $\bar{\nu}_e$ spectra for scalar, pseudoscalar and tensorial NSI at some specific coupling parameters using CsI(Tl) as a target.

like or so called zero-distance interaction. Feynman diagram of different NSI for neutrino-electron scattering is illustrated schematically in Fig. 1.

Both neutrino oscillation and non-oscillation experiments are sensitive to NSI parameters and can give complementary results. Non-oscillation neutrino experiments provide direct measurement of NSI while neutrino oscillation experiments are more sensitive to propagation of NSI parameters due to matter effects [4]. NSI can simply be considered as modification of coupling constants with additional new terms to the chiral couplings of $g_{L,R}$ in general.

Phenomenological studies of Flavor-Conserving (FC) and Flavor-Violating (FV) NSI of neutrino have been extensively carried out with a variety of interaction channels and neutrino sources [16–21]. Experimentally new bounds for FC coupling of $\varepsilon^{eL,R}_{ee}$ and FV coupling of $\varepsilon^{eL,R}_{e\tau}$ NSI parameters were derived and existing bounds were improved in our earlier work by taking advantages of neglecting oscillation effects and high neutrino flux [6]. On the other hand, other NSI of neutrino are also possible which are scalar, pseudoscalar and spin-2 tensorial type.

Observing of NSI would imply the existence of right-handed neutrinos, therefore, it is an important channel to study new physics BSM. However, there are few studies exist on scalar, pseudoscalar or tensorial type NSI in the literature mainly due to motivation of V-A structure of SM and the assumption of their small contributions to the cross-section. To overcome this deficiency, in addition to FC and FV NSI parameters scalar, pseudo-scalar, and tensorial NSI of neutrino are studied via (anti)neutrino-

Table I. Summary of best fit results and corresponding limits at %90 CL for scalar, pseudoscalar and tensorial NSI measurements for one parameter at a time analysis for ν_e- and $\bar{\nu}_e - e$ scattering.

NSI Parameters	TEXONO Measurement Best-Fit (1-σ)	χ^2/dof	TEXONO Bounds at 90% CL	LSND Measurement Best-Fit (1-σ)	LSND Bounds at 90% CL
Scalar $g_S^{e,e}$ ($g_P^{e,e}=0$)	$g_S^{e,e} = [3.27 \pm 6.39 \pm 3.10] \times 10^{-2}$	8.7/9	$-0.317 < g_S^{e,e} < 0.113$	$g_S^{e,e} = 0.27 \pm 0.59 \pm 0.26$	$-0.880 < g_S^{e,e} < 0.642$
Pseudoscalar $g_P^{e,e}$ ($g_S^{e,e}=0$)	$g_P^{e,e} = [-3.27 \pm 6.39 \pm 3.10] \times 10^{-2}$	8.7/9	$-0.113 < g_P^{e,e} < 0.317$	$g_P^{e,e} = -0.27 \pm 0.59 \pm 0.26$	$-0.642 < g_P^{e,e} < 0.880$
$g_{S=P}^{e,e}$ ($g_S^{e,e}=g_P^{e,e}$)	$(g_{S=P}^{e,e})^2 = [0.19 \pm 0.38 \pm 0.31] \times 10^{-2}$	8.7/9	$\lvert g_{S=P}^{e,e}\rvert < 0.100$	$(g_{S=P}^{e,e})^2 = [3.47 \pm 4.78 \pm 4.36] \times 10^{-2}$	$\lvert g_{S=P}^{e,e}\rvert < 0.375$
Tensorial $g_T^{e,e}$	$(g_T^{e,e})^2 = [0.96 \pm 2.21 \pm 1.82] \times 10^{-2}$	8.7/9	$\lvert g_T^{e,e}\rvert < 0.238$	$(g_T^{e,e})^2 = [3.96 \pm 5.47 \pm 4.97] \times 10^{-2}$	$\lvert g_T^{e,e}\rvert < 0.401$

electron interaction channel and new limits are set to the related parameters by adopting a model independent method introduced in this paper.

The effective Lagrangian for scalar and/or pseudoscalar interaction [22] can be written as

$$\mathcal{L}_{S,P} = \sum_{\alpha}\sum_{\beta} \bar{l}_\alpha \left(\mathcal{O}_{S,P}\right) \nu_\beta \ , \tag{5}$$

where $(\mathcal{O}_{S,P})$ is a general operator with scalar/pseudoscalar interactions.

The effective Lagrangian for tensorial NSI [23] interaction can be written as

$$-\mathscr{L}_{\rm T}^{\rm eff} = \varepsilon_{\alpha\beta}^{fT} 2\sqrt{2} G_F (\bar{\nu}_\alpha \sigma^{\mu\nu} \nu_\beta)(\bar{f}\sigma_{\mu\nu} f) \tag{6}$$

with $\sigma^{\mu\nu} = [\gamma^\mu, \gamma^\nu] = \gamma^\mu\gamma^\nu - \gamma^\nu\gamma^\mu$ and $\alpha, \beta = e,\ \mu,\ \tau$.

The differential cross section of scalar-pseudoscalar NSI interaction for $\nu_e - e^-$ and $\bar{\nu}_e - e^-$, respectively, can be written as

$$\left[\frac{d\sigma_{\nu_e,e}}{dT}\right]_{\rm S,P}^{\rm NSI} = \frac{2G_F^2 m_e}{\pi}\left\{\left[(|g_S^{e,e}| + |g_P^{e,e}|)^2 + g_R {\rm Re}\left(g_S^{e,e} - g_P^{e,e}\right)\right]\left(1 - \frac{T}{E_\nu}\right)^2 - (g_L+1)\,{\rm Re}\left(g_S^{e,e} - g_P^{e,e}\right)\frac{m_e T}{2E_\nu^2}\right\} \tag{7}$$

and

$$\left[\frac{d\sigma_{\bar{\nu}_e,e}}{dT}\right]_{\rm S,P}^{\rm NSI} = \frac{2G_F^2 m_e}{\pi}\left\{(|g_S^{e,e}| + |g_P^{e,e}|)^2 + g_R {\rm Re}\left(g_S^{e,e} - g_P^{e,e}\right) - (g_L+1)\,{\rm Re}\left(g_S^{e,e} - g_P^{e,e}\right)\frac{m_e T}{2E_\nu^2}\right\} . \tag{8}$$

In the tensorial NSI case there will be no interference between SM interaction channels of neutral- and charged-current since incoming and outgoing neutrino's helicities would be different at the exchange vertex. In that case the contribution of tensorial interaction to the SM cross section should be just added numerically. The differential cross section of tensorial NSI interaction can be written as [10, 23]

$$\left[\frac{d\sigma}{dT}\right]_{\rm T}^{\rm NSI} = \frac{2G_F^2 m_e}{\pi}\sum_{\beta=e,\mu,\tau}\left(\varepsilon_{e\beta}^{eT}\right)^2\left[2\left(1 - \frac{T}{2E_\nu}\right)^2 - \frac{m_e T}{2E_\nu^2}\right] , \tag{9}$$

where $\varepsilon_{e\beta}^{eT}$ is the strength of the tensorial NSI coupling on electrons.

Since we will only consider one parameter at a time in the analysis and the contribution of ε_{ee}^{eT} is the same as $\varepsilon_{e\beta}^{eT}$ for $\beta \neq e$ case, so we will denote $\varepsilon_{e\beta}^{eT}$ as $g_T^{e,e}$ along the paper same as in the literature.

The measurable recoil spectra at a typical reactor flux of $\phi(\bar{\nu}_e) = 10^{13}$ cm^{-2}s^{-1} are displayed in Fig. 2 for a typical scalar, pseudo-scalar and tensorial NSI parameters. The NSI contributions for all type give rise to quite similar spectral shapes with the SM ones. Accordingly, like FC and FV NSI, the most suitable energy range to study scalar, pseudo-scalar and tensorial NSI is in MeV energy range where the SM effects were measured with good accuracies.

Like the FC and FV NSI parameters, the scalar, pseudoscalar and tensorial NSI parameters [23–25] are also constrained by the accuracy of the SM cross section measurements. Accordingly, only CsI(Tl) data set for TEXONO and LSND Experiment are adopted for scalar, pseudo-scalar and tensorial NSI analysis.

The scalar and pseudoscalar NSI parameters $g_{S,P}^{e,e}$ given in Eq. (7) and Eq. (8) are the fitting variables in the minimum-χ^2 analysis. If $g_S^{e,e} = g_P^{e,e}$ then there will be some simplifications in these equations. In this case $(g_{S=P}^{e,e})^2$ becomes the fitting parameter.

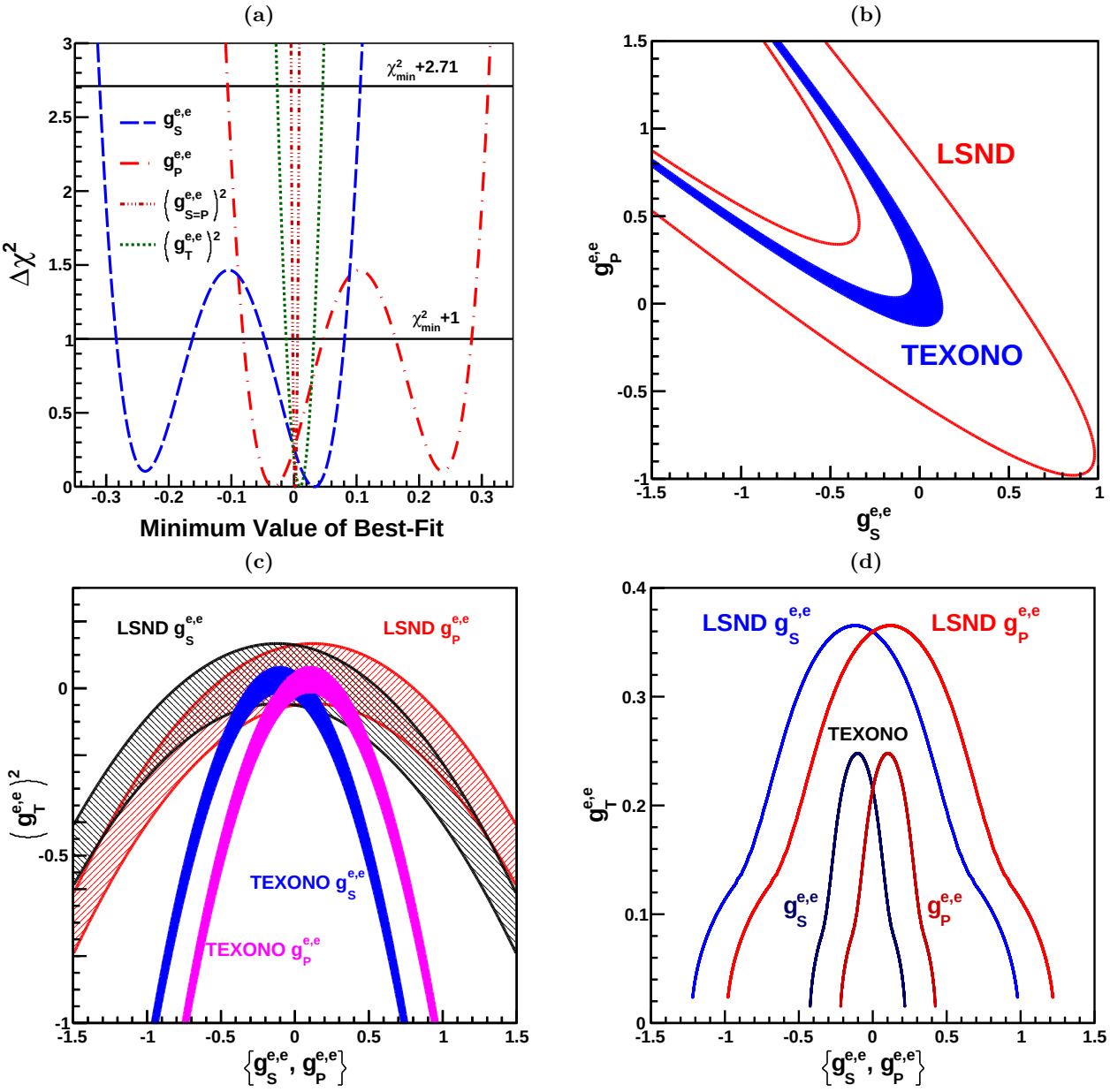

Figure 3. (color online). (a) $\Delta\chi^2$ of one parameter at a time analysis for $g^{ee}_{S,P}$, $(g^{e,e}_{S=P})^2$ and $(g^{e,e}_T)^2$. The allowed region at 90% CL for TEXONO and LSND Experiments in (b) $g^{e,e}_S - g^{e,e}_P$, (c) $g^{e,e}_S - (g^{e,e}_T)^2$ and $g^{e,e}_P - (g^{e,e}_T)^2$ parameter spaces. (d) Upper limits at 90% CL of $g^{e,e}_T$ as functions of $g^{e,e}_S$ and $g^{e,e}_P$.

By adopting one parameter at a time analysis, from the best-fit

$$\begin{aligned} g^{e,e}_S &= [3.27 \pm 6.39 \pm 3.10] \times 10^{-2} \ , \\ g^{e,e}_P &= [-3.27 \pm 6.39 \pm 3.10] \times 10^{-2} \ , \\ (g^{e,e}_{S=P})^2 &= [0.19 \pm 0.38 \pm 0.31] \times 10^{-2} \ \text{, and} \\ (g^{e,e}_T)^2 &= [0.96 \pm 2.21 \pm 1.82] \times 10^{-2} \end{aligned} \quad (10)$$

are obtained at $\chi^2_{min}/\text{dof} = 8.7/9$.

These results are converted to the bounds for the scalar and pseudo-scalar NSI but only upper limits for tensorial and $|g^{e,e}_{S=P}|$ NSI couplings as

$$\begin{aligned} -0.317 < g^{e,e}_S < 0.113 \ \ (\text{for} \ \ g^{e,e}_P = 0) \ \ , \\ -0.113 < g^{e,e}_P < 0.317 \ \ (\text{for} \ \ g^{e,e}_S = 0) \ \ , \\ |g^{e,e}_{S=P}| < 0.100 \ \ (\text{for} \ \ g^{e,e}_S = g^{e,e}_P) \ \ \text{, and} \\ g^{e,e}_T < 0.238 \ \ (\text{for} \ \ g^{e,e}_S = g^{e,e}_P = 0) \end{aligned} \quad (11)$$

at 90 % CL for TEXONO CsI(Tl) data set.

The best fit results and χ^2 behaviours of the scalar, pseudoscalar and tensorial NSI parameters of $g^{ee}_{S,P}$,

$(g_{S=P}^{e,e})^2$ and $(g_T^{e,e})^2$ which are adopted as fitting variables are illustrated in Fig. 3(a).

Similarly,

$$\begin{aligned} g_S^{e,e} &= 0.27 \pm 0.59 \pm 0.26, \\ g_P^{e,e} &= -0.27 \pm 0.59 \pm 0.26, \\ (g_{S=P}^{e,e})^2 &= [3.47 \pm 4.78 \pm 4.36] \times 10^{-2} \quad , \text{and} \\ (g_T^{e,e})^2 &= [3.96 \pm 5.47 \pm 4.97] \times 10^{-2} \end{aligned} \tag{12}$$

are derived for LSND Experiment and they correspond to the limits of

$$\begin{aligned} -0.880 < g_S^{e,e} < 0.642 \quad &(\text{for} \quad g_S^{e,e} = 0), \\ -0.642 < g_P^{e,e} < 0.880 \quad &(\text{for} \quad g_P^{e,e} = 0), \\ |g_{S=P}^{e,e}| < 0.375 \quad &(\text{for} \quad g_S^{e,e} = g_P^{e,e}) \quad , \text{and} \\ g_T^{e,e} < 0.401 \quad &(\text{for} \quad g_S^{e,e} = g_P^{e,e} = 0) \end{aligned} \tag{13}$$

at 90 % CL which are similar to published results of LAMPF Experiment reported in Ref. [26] since their experimental sensitivities are similar.

The results of one parameter at a time analysis for TEXONO and LSND Experiments are listed in Table I. As can be seen that TEXONO CsI(Tl) data set provides much better constraints than those from LSND or LAMPF accelerator experiments and also from the other reactor neutrino experiment data sets given in Ref. [23].

The allowed regions at 90% CL from two-parameter analysis in the ($g_{S,P}^{e,e}$ and $(g_T^{e,e})^2$) parameter spaces are displayed in Fig. 3 in which LSND results are superimposed for complementarity. The 90% CL upper limits of $g_T^{e,e}$ as functions of $g_S^{e,e}$ and $g_P^{e,e}$ for the two experiments are displayed in Fig. 3(d). It can be seen that the TEXONO data provides more stringent constraints than those from LSND in both the $g_S^{e,e} - g_P^{e,e}$ and $g_{S,P}^{e,e} - g_T^{e,e}$ parameter spaces.

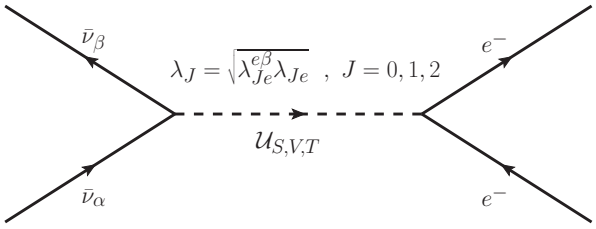

Figure 4. Interactions of neutrino with electron via exchange of massive mediators such as virtual unparticle (scalar $\mathcal{U}_\mathcal{S}$, vector $\mathcal{U}_\mathcal{V}$ or tensorial $\mathcal{U}_\mathcal{T}$).

IV. UNPARTICLE PHYSICS

Unparticle physics was first presented by Georgi with two articles in 2007. Besides SM fields, a sector is assumed to be scale invariant at high energies. These fields are called Banks-Zaks ($\mathcal{BZ}$) fields. In this model SM

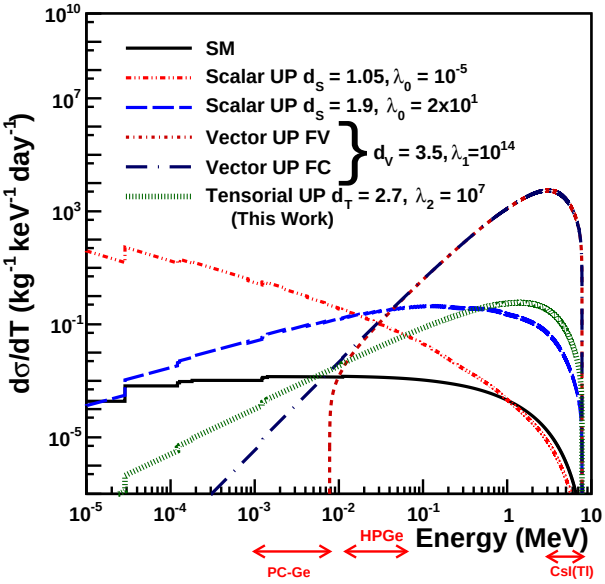

Figure 5. (color online). Differential cross section as a function of the recoil energy T with typical reactor $\bar{\nu}_e$ spectra for scalar UP at two values of $(d_\mathcal{S}, \lambda_0)$, for vector UP at a value of $(d_\mathcal{V}, \lambda_1)$ for both Flavor-Violating (FV) and Flavor-Conserving (FC) UP cases [6], and for tensorial UP at a value of (d_T, λ_2) (This Work). The relevant energy ranges of the three data sets used in the present analysis are also shown.

fields interact with $\mathcal{BZ}$ fields by an exchange of mass scale invariant massive particles that are called unparticle [27, 28].

The effective Lagrangian is given by [23, 29]

$$\mathcal{L}_\mathcal{U} = C_{\mathcal{O}_\mathcal{U}} \frac{\Lambda_\mathcal{U}^{d_{\mathcal{BZ}} - d_\mathcal{U}}}{M_\mathcal{U}^{d_{\mathcal{SM}} + d_{\mathcal{BZ}} - 4}} \mathcal{O}_{\mathcal{SM}} \mathcal{O}_\mathcal{U} \ , \tag{14}$$

where $\mathcal{O}_\mathcal{U}$ is the unparticle operator of scaling dimension $d_\mathcal{U}$ in the low energy limit and $C_{\mathcal{O}_\mathcal{U}}$ is dimensionless coupling constant. The unparticle operator can be a scalar, vector, spinor, or tensor type.

Unparticle can directly be studied in accelerator experiments via investigating missing energy signals in the detection channel [30], but alternatively its effect can also be examined in neutrino-electron elastic scattering channel as being a virtual mediator particle. Latter approach is adopted in this analysis using reactor neutrinos as probes. Scalar and Vector UP for both Flavor-Violating (FV) and Flavor-Conserving (FC) cases are studied in our early work [6], in this paper we focus on Tensorial UP interaction.

The interaction Lagrangian for $\nu_\alpha + e \to \nu_\beta + e$ depicted in Fig. 4 via tensorial unparticle exchange are given by [30–35]

$$\begin{aligned} \mathscr{L}_{\text{J=2}} = &\frac{-i}{4} \frac{\lambda_{2e}}{\Lambda_\mathcal{U}^{d_\mathcal{T}}} \bar{e} \left(\gamma_\mu \overleftrightarrow{D}_\nu + \gamma_\nu \overleftrightarrow{D}_\mu \right) \psi_e \mathcal{O}_\mathcal{U}^{\mu\nu} \\ &+ \frac{\lambda_{2\nu}^{\alpha\beta}}{\Lambda_\mathcal{U}^{d_\mathcal{T}}} \mathcal{F}_{\mu\alpha} \mathcal{F}_\nu^\alpha \mathcal{O}_\mathcal{U}^{\mu\nu} \ , \end{aligned} \tag{15}$$

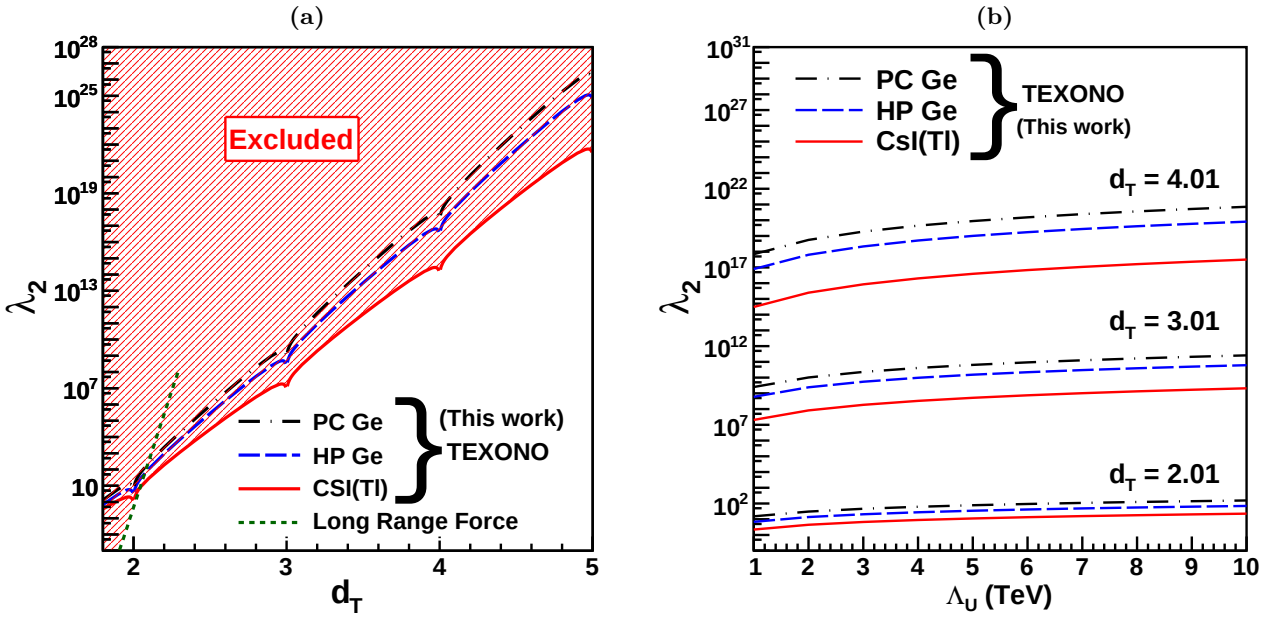

Figure 6. (color online). Constraints on UP with tensorial exchange (a) The coupling λ_2 versus mass dimension d_T at $\Lambda_U = 1$ TeV for the three data sets adopted for this analysis in which long range force result is superimposed for comparison. (b) Upper bounds on λ_2 at different energy scales Λ_U. The space above the lines is excluded.

where $\mathcal{F}_{\mu\nu}$ is the gauge field strength and λ_{2e} and $\lambda_{2\nu}^{\alpha\beta}$ are the corresponding coupling constants.

The cross section of $\bar{\nu}_e - e$ scattering via tensorial UP exchange is given by [23]

$$\left(\frac{d\sigma}{dT}\right)_{\mathcal{U}_T} = \frac{f^2(d_T)}{\pi\Lambda_{\mathcal{U}}^{4d_T-4}}\, 2^{2d_T-3}\, m_e^{2d_T-3}\, T^{2d_T-4} \times \left[3\left(1-\frac{T}{2E_\nu}\right)^2 - \frac{m_e T}{2E_\nu^2}\right], \quad (16)$$

where

$$f(d_X) = \frac{\lambda_X^2}{2\sin(d_X\pi)} A(d_X) \quad (17)$$

and the normalization constant $A(d_X)$ is given by

$$A(d_X) = \frac{16\pi^{5/2}}{(2\pi)^{2d_X}} \frac{\Gamma(d_X+1/2)}{\Gamma(d_X-1)\Gamma(2d_X)}\,. \quad (18)$$

The cross section of $\bar{\nu}_e - e$ scattering via all kind of UP exchange can be obtained by making a replacement of $d_X \to d_S, d_V$ or d_T and $\lambda_X \to \lambda_0, \lambda_1$ or λ_2 representing scalar, vector and tensorial UP interaction, respectively.

The differential cross sections of scalar, both FC and FV vector and tensor type UP interaction at a typical mass dimension of d using TEXONO CsI(Tl), HP-Ge and PC-Ge detector data sets are displayed in Fig. 5, where SM contribution is superimposed for comparison. The sawtooth structures for $T \lesssim 1$ keV are due to suppression by the atomic binding energy [8, 36]. As illustrated in the figure the cross sections of different UP type give different behavior with respect to the recoil energy.

Working at high energy regime has much more advantage than at low energy in the case of tensorial UP which is the same as both FC and FV vector UP, and for scalar UP with higher mass dimension of d. On the other hand, low energy regime is more favorable for scalar UP with low mass dimension of d. Since the cross sections of the SM is measured more precisely in MeV energy range, more sensitive results are expected for tensorial UP with CsI(Tl) detector data set compare to those from Ge detector data sets. Since different ranges of d_T for all the data sets listed above give different and comparable sensitivities, all the three data sets of $\bar{\nu}_e - e$ are used in the tensorial UP analysis for their complementarity.

Three parameters, unparticle mass dimension d_T, unparticle energy scale Λ_U and coupling constant $\lambda_2 \equiv \sqrt{\lambda_{2\nu}^{e\beta}\lambda_{2e}}$ characterizing the unparticle interactions can be probed experimentally. There is a bound on d_T as $d_T \geq 2$ for anti-symmetric tensor and $d_T \geq 4$ for the symmetric case [37]. The UP energy scale is taken to be $\Lambda_{\mathcal{U}} \sim 1$ TeV as in most recent works [32, 33, 38] as well as $\Lambda_{\mathcal{U}}$ up to 10 TeV.

Constraints on λ_2 at different d_T in the case of tensorial UP exchange interaction are derived at $\Lambda_U = 1$ TeV. The results are shown in Fig. 6(a) in which long range force result reported in Ref. [33] is superimposed for comparison.

In order to observe UP signal from the data and to set bounds on it, among the investigations of the collider, CP violation, deep-inelastic, lepton flavor violating, hadron mixing and decay, neutrino interaction, nucleon decay experiments and cosmological and astroparticle efforts

there is another unparticle approach that is long-range forces operating at macroscopic distances and governed by a non-integral power law which was first introduced in Ref. [39]. It is based on spin-dependent interactions between electrons and related to the Newtonian gravitational inverse squared law mediated by a tensor-like ungravity interaction [40].

The upper bounds for λ_2 at different energy scale Λ_U up to 10 TeV are shown in Fig. 6(b). As can be seen, the limits are improved by TEXONO CsI(Tl) data set for $d_T > 2.04$, CsI(Tl) gives rise to more stringent limits at larger d_T.

Since $(d\sigma/dT)_{\mathcal{U}_\mathcal{T}}$ is proportional to λ_2^4 which can be seen from Eq. (16), the potential of placing more severe constraints on the coupling constants due to improved experimental sensitivities can only be modest. When CsI(Tl) data would improve to provide a 1% measurement of the SM cross section and similarly, sub-keV Ge data with a 1% improvement in the experimental sensitivities of ON-OFF subtraction [41], an improvement by a factor of around 3 can be expected to the sensitivity of λ_2.

V. SUMMARY AND PROSPECTS

In summary of this article, some of the model independent BSM new physics scenarios such as scalar, pseudoscalar, and tensorial NSI and tensorial component of Unparticle Physics are discussed. The investigation on the neutrino oscillation phenomena came to more and more precision era. Therefore, the existence and contribution of NSI would help to increase the precision of the experiments.

The experimental results of upper bounds for NSIs using data from the analysis of $\bar{\nu}_e - e$ and $\nu_e - e$ elastic scattering interaction cross section measurements are placed in the frame work of these BSM scenarios and the existing experimental sensitivities are improved. We have found new constraints on the relevant parameters that are more stringent than previous laboratory constraints.

Indeed, TEXONO provides better sensitivity in NSI parameter space compare to LSND Experiment, therefore combined results will improve the existing bounds. Moreover, with this study we extend the parameter space as well with covering low mass dimension of d in UP physics studies.

A new research channel prompts to investigate of BSM theories can be opened via $\bar{\nu}_e$-nucleus coherent scattering that is in the part of the TEXONO low-energy neutrino physics road map program.

VI. ACKNOWLEDGMENTS

This work is supported by contract 114F374 under TUBITAK, Turkey and 104-2112-M-001-038-MY3 from the Ministry of Science and Technology, Taiwan.

[1] S.F. King, Journal of Physics G: Nuclear and Particle Physics **42(12)**, 123001 (2015).
[2] J. Panman, in *Precision tests of the standard electroweak model*, ed. P. Langacker, 504-544, World Scientific (1995); W.J. Marciano and Z. Parsa, J. Phys. G **29**, 2629 (2003).
[3] T. Nilsson, Reports on Progress in Physics **76(4)**, 044201 (2013).
[4] O.G. Miranda and H. Nunokawa, New Journal of Physics **17(9)**, 095002 (2015).
[5] J. Erler and P. Langacker, Phys. Lett. B **667**, 125 (2008), and references therein.
[6] M. Deniz *et al.*, Phys. Rev. D **82**, 033004 (2010).
[7] S. Bilmiş *et al.*, Phys. Rev. D **85**, 073011 (2012).
[8] J.W. Chen, H.C. Chi, H.B. Li, C.P. Liu, L. Singh, H.T. Wong, C.L. Wu, and C.P.Wu, Phys. Rev. D **90**, 011301(R) (2014).
[9] S. Bilmis, I. Turan, T.M. Aliev, M. Deniz, L. Singh, and H.T. Wong, Phys. Rev. D **92**, 033009 (2015).
[10] B. Kayser, E. Fischbach, S.P. Rosen, and H. Spivack, Phys. Rev. D **20**, 87 (1979).
[11] M. Deniz *et al.*, Phys. Rev. D **81**, 072001 (2010).
[12] H.B. Li *et al.*, Phys. Rev. Lett. **90**, 131802 (2003); H.T. Wong *et al.*, Phys. Rev. D **75**, 012001 (2007).
[13] A.K. Soma *et al.*, Nucl. Instr. and Meth. **A 836**, 67 (2016).
[14] L.B. Auerbach *et al.*, Phys. Rev. D **63**, 112001 (2001).
[15] Gary J. Feldman and Robert D. Cousins, Phys. Rev. D **57**, 3873 (1998).
[16] N. Fornengo, M. Maltoni, R.T. Bayo and J.W.F. Valle, Phys. Rev. D **65**, 013010 (2001); P.S. Amanik, G.M. Fuller and B. Grinstein, Astropart. Phys. **24**, 160 (2005); G.L. Fogli, E. Lisi, A. Mirizzi and D. Montanino, Phys. Rev. D **66**, 013009 (2002); A. Esteban-Pretel, R. Tomas and J.W.F. Valle, Phys. Rev. D **76**, 053001 (2007).
[17] O.G. Miranda, M. Maya and R. Huerta, Phys. Rev. D **53**, 1719 (1996); O.G. Miranda, V. Semikoz and J.W.F. Valle, Nucl. Phys. Proc. Suppl. **66**, 261 (1998); J. Barranco, O.G. Miranda and T.I. Rashba, Phys. Rev. D **76**, 073008 (2007); A. Bolanos *et al.*, Phys. Rev. D **79**, 113012 (2009).
[18] S. Davidson *et al.*, JHEP **0303**, 011 (2003).
[19] J. Barranco *et al.*, Phys. Rev. D **73**, 113001 (2006); J. Barranco *et al.*, Phys. Rev. D **77**, 093014 (2008).
[20] C. Biggio, M. Blennow, and E. Fernandez-Martinez, JHEP **03**, 139 (2009); C. Biggio, M. Blennow, and E. Fernandez-Martinez, JHEP **08**, 090 (2009).
[21] J. Barranco, O.G. Miranda and T.I. Rashba, JHEP **0512**, 021 (2005); K. Scholberg, Phys. Rev. D **73**, 033005 (2006).
[22] R. Gaitan *et al.*, Int. J. Mod. Phys. A **28**, 1350124 (2013).

[23] J. Barranco *et al.*, Int. J. Mod. Phys. A **27**, 1250147 (2012).

[24] K.J. Healey, A.A. Petrov, D. Zhuridov, Phys. Rev. D **87** (2013) 117301.

[25] D.K. Papoulias and T.S. Kosmas, Phys.Lett. B **747** (2015).

[26] R.C. Allen *et al.*, Phys. Rev. D **47**, 11 (1993).

[27] H. Georgi, Phys. Rev. Lett. **98**, 221601 (2007); H. Georgi, Phys. Lett. B **650**, 275 (2007).

[28] A. Lenz, Phys. Rev. D **76**, 065006 (2007).

[29] A. Bolaos, *et al.*, Phys. Rev. D **87(1)**, 016004 (2013).

[30] K. Cheung, W.Y. Keung, and T.C. Yuan, Phys. Rev. Lett. **99**, 051803 (2007); K. Cheung, W.Y. Keung, and T.C. Yuan, Phys. Rev. D **76**, 055003 (2007).

[31] S.L. Chen and X.G. He, Phys. Rev. D **76**, 091702 (2007).

[32] A.B. Balantekin and K.O. Ozansoy, Phys. Rev. D **76**, 095014 (2007).

[33] J. Barranco *et al.*, Phys. Rev. D **79**, 073011 (2009).

[34] E.A. Garcés *et al.*, J. Phys. Conf. Ser. **378**, 012017 (2012).

[35] T.I. Hur, P. Ko and X.H. Wu, Phys. Rev. D **76**, 096008 (2007).

[36] S.A. Fayans, L.A. Mikaelyan and V.V. Sinev, Phys. Atom. Nucl. **64**, 1475 (2001); M. B. Voloshin, Phys. Rev. Lett. **105**, 201801 (2010), erratum: ibid. 106, 059901 (2011); J.W. Chen, H.C. Chi, K.N. Huang, C.P. Liu, H.T. Shiao, L. Singh , H.T. Wong, C.L. Wu and C.P. Wu, Phys. Lett. B **731**, 159 (2014); J.W. Chen, H.C. Chi, K.N. Huang, H.B. Li, C.P. Liu, L. Singh , H.T. Wong, C.L. Wu and C.P. Wu, Phys. Rev. D **91**, 013005 (2015); J.W. Chen, H.C. Chi, S.T. Lin, C.P. Liu, L. Singh, H.T. Wong, C.L. Wu and C.P. Wu, Phys. Rev. D **93**, 093012 (2016).

[37] B. Grinstein, K. Intriligator and I. Z. Rothstein, Phys. Lett. B **662**, 367 (2008).

[38] D. Montanino, M. Picariello and J. Pulido, Phys. Rev. D **77**, 093011 (2008).

[39] Yi Liao and Ji-Yuan Liu, Phys. Rev. Lett. **99**, 191804 (2007).

[40] M.C. Gonzalez-Garcia, P.C. Holanda and R. Zukanovich Funchal, J. Cosmol. Astropart. Phys. **2008** (2008).

[41] H.T. Wong *et al.*, J. Phys. Conf. Ser. **39**, 266 (2006).